ISSN 2176-5480

22nd International Congress of Mechanical Engineering (COBEM 2013)
November 3-7, 2013, Ribeirão Preto, SP, Brazil

VALIDATION OF A NUMERICAL VEHICLE MODEL WITH 10 DEGREES OF FREEDOM USING THE ANALYTICAL MODEL

Adriano Nicholls Couto
Pedro Henrique de Castro e Aquino
Lúcio Flávio dos Santos Patrício
Janes Lándre Júnior
Pontifícia Universidade Católica de Minas Gerais, Belo Horizonte
adrianonicholls@hotmail.com
pedro.eng2011@hotmail.com
luciopatricio@pucminas.br
janes@pucminas.br

Abstract. *This paper deals with the development of an analytical model of a vehicle with 10 degrees of freedom, and their numerical implementation. There will be developed equations of motion that govern the system and then this model is implemented in MATLAB®. The model will also be implemented in commercial software ADAMS/VIEW®. The results obtained in tests with software and analytical model will be compared with the results obtained in the analytical model in order to validate the numerical simulations.*

Keywords: *analytical model, vehicle dynamics, multi-body simulation , numerical vehicle model*

1. ROAD VEHICLE DYNAMICS

The road vehicle dynamics is divided into two areas: isolation and control. The first area is concerned with isolating the passenger disturbances caused by vibration sources that act on the structure of the vehicle. The second area is concerned with the vehicle response to driver input through the steering wheel (Blundell and Harty, 2004). Isolation is divided into internal and external sources of vibration, as shown in Figure 1.

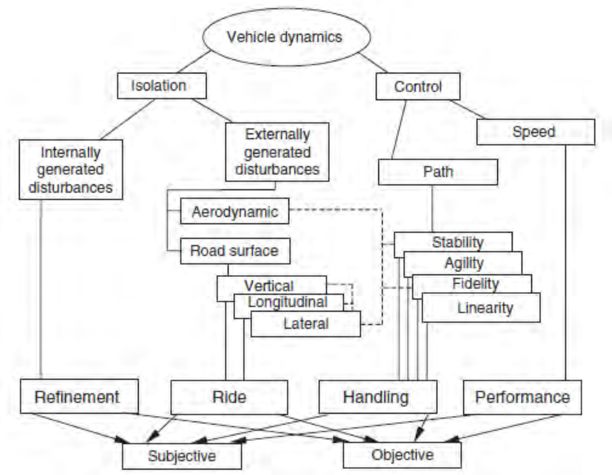

Figure 1. Structure of vehicle dynamics – Blundell and Harty, 2004

According to Gillespie (1992) the road vehicles in travelling at a known speed experience a wide spectrum of vibrations transmitted by different sources. Genta (2009) divides vibrations source in two groups: internal sources and external sources. External sources included road roughness and aerodynamic effects. Internal sources included the movement of the rotating parts of the engine and their possible imbalance mass, movement of the components to the driveline system, dimensional and geometric variations of the tire/wheel assembly and the stiffness variation along the tire structure. These vibration are transmitted to the passenger through the vehicle structure and can be felt by tactile, aural and visually (Gillespie, 1992). According to Reimpell, (2001) the stiffness variation along the tire should vary 5%, otherwise the dynamic radius is affected and this causes a great variation in the vertical force along de contact between tire and pavement. (Dukkipati *et al*, 2008) shows vibrations arising from contact between tire/track depends on the profile of the track, velocity of travelling and the dynamic properties of the tire. The level of acceleration in the tire/wheel assembly is proportional at the square of travelling velocity of vehicle, i.e., the input frequency in the system increases with speed (Gillespie, 1992). The vertical dynamics of the vehicle is a medium for the natural frequencies and acceleration levels in each body.

The comfort analysis is performed using the concept of the ride comfort. The ride comfort is the analysis of how passengers can be felt this vibration from the road roughness and check if this level of vibration does not cause discomfort (Stone and Ball, 2004). Ride comfort analyzes only tactile and visual vibration, while the aural vibrations are considered noise. The ride comfort range frequency varies between 0 and 20 Hz, and that for frequencies from 0 to 5 Hz is the so-called primary ride and for frequencies from 5 a 20 Hz is the so-called second ride. The sprung mass natural frequencies are in the primary ride and the other components of the vehicle in the second ride. Passenger vehicles commonly have natural bounce frequency around 0.9 to 1.1 Hz natural frequency pitch around 1 to 1.5 Hz and roll around 1.5 to 2 Hz (Wong, 2001). According to Griffin (2009) the development of dynamic models is a powerful tool for ride comfort analysis, because it provides the acceleration time history in various axes of vibration and different vibrations in different locations of vehicle structure. Also, allow objective evaluations of ride comfort subjective evaluations complementing the passenger.

Vibrations can cause a lot of disturbances on the human body and its effects can be permanent or transient. The perception of these effects varies from one person against other; therefore the analysis of ride comfort is a subjective concept. The acceleration levels caused by these vibrations can be measured by analytical method, numerical simulations or experimental methods (Griffin, 2009).

2. FULL CAR MODEL

The full car model is based on the model purpose for Patrício (2005) and Bouazara (2001). The first model has 7 degrees of freedom and considers the action of front and rear antiroll bar. The second model has 8 degrees of freedom and considers the vertical acceleration of driver seat. The objective of Bouazara is study a comfort zone without affecting road holding capability.

Figure 2 shows the 3-D vehicle model implemented in ADAMS/VIEW®. This model considers the degrees of freedom relative to the vertical movement of seat and of the driver body and the driver head. Both in ADAMS/VIEW® and MATLAB® the wheelbase is asymmetric. The position of the seat was established at 0.1 m distance in axis x and y, relative to the CG of the sprung mass.

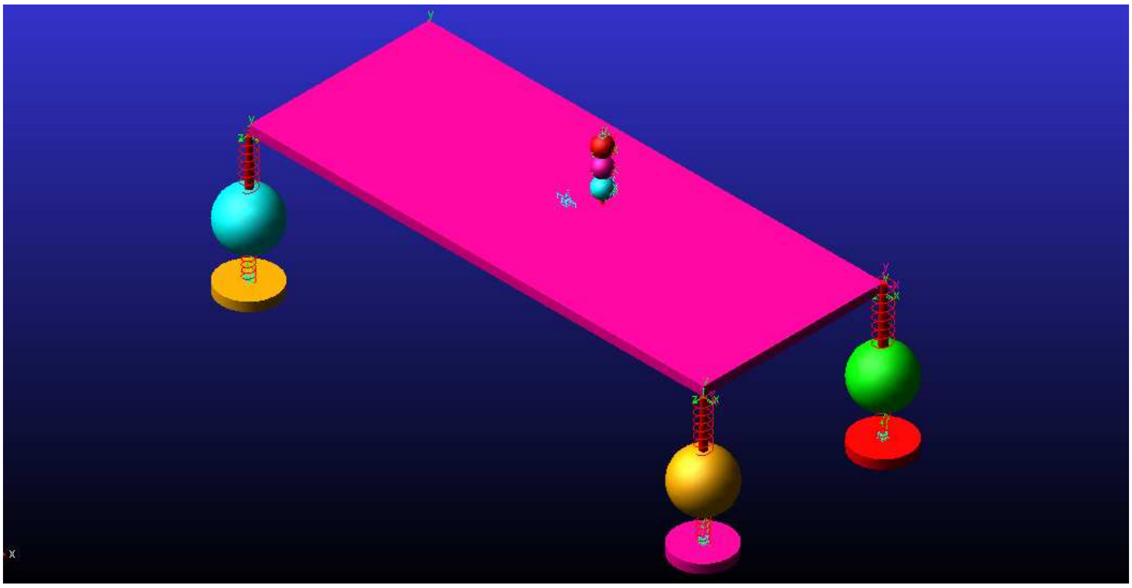

Figure 2. 3-D vehicle model with 10 degrees of freedom modeled in ADAMS/VIEW®

Table 1 shows the mass, spring stiffness and damping coefficient of each component of the system. There were used the same values in both software MATLAB® and ADAMS/VIEW®.

ISSN 2176-5480

Table 1. Properties of the rigid bodies

Part	**Value**
Unsprung mass	50 Kg
Sprung mass	1513 Kg
Sprung mass inertia in direction x	637.26 Kg*m^2
Sprung mass inertia in direction z	2443.26 Kg*m^2
Driver head mass	5.5 Kg
Driver body mass	63 Kg
Seat mass	7.7Kg
Suspension stiffness	15000N/m
Suspension damping	200 Ns/m
Seat stiffness	13000 N/m
Seat damping	50 Ns/m
Tire stiffness	150000 N/m
Driver Head stiffness	13000 N/m
Driver Head damping	50 Ns/m
Driver Body stiffness	13000 N/m
Driver Body damping	50 Ns/m

Table 2 shows the vehicle dimensions in meters.

Table 2. Vehicle Dimensions

Distance from CG to front axle	1.2218
Distance from CG to rear axle	1.2886
Inner wheel	0.500
Outer wheel	0.500

In this paper some simplifications were established:

- The contact between tire and the road is permanent
- The parts have vertical movement and rotation of the sprung mass in the axis x and z
- Parties concerning the pavement have no mass and moments of inertia

The equations of motion obtained for this model are presented below.

$$m_H \ddot{z}_H + K_H z_H - K_H z_c + C_H \dot{z}_H - C_H \dot{z}_c = 0 \tag{1}$$

$$m_c \ddot{z}_c + (K_H + K_c) z_c - K_c z_b - K_H z_H + (C_H + C_c)\dot{z}_c - C_c \dot{z}_b - C_H \dot{z}_H = 0 \tag{2}$$

$$\begin{aligned} & m_b \ddot{z}_b + (K_b + K_c) z_b - K_b z_s + x_{banco} K_b \theta_s - y_{banco} K_b \varphi_s - K_c z_c + (C_b + C_c)\dot{z}_b - C_b \dot{z}_s \\ & + x_{banco} C_b \dot{\theta}_s - y_{banco} C_b \dot{\varphi}_s - C_c \dot{z}_c = 0 \end{aligned} \tag{3}$$

$$\begin{aligned} & M_s \ddot{z}_s + (K_{s1} + K_{s2} + K_{s3} + K_{s4} + K_{banco}) z_s + (-l_d K_{s1} - l_d K_{s2} + l_t K_{s3} + l_t K_{s4} - x_{banco} K_{banco})\theta_s \\ & - K_{s1} z_{u1} - K_{s2} z_{u2} - K_{s3} z_{u3} - K_{s4} z_{u4} + (-b_{d1} K_{s1} + b_{d2} K_{s2} + b_{t2} K_{s3} - b_{t2} K_{s4} + y_{banco} K_{banco})\varphi_s \\ & - K_{banco} z_{banco} + (C_{s1} + C_{s2} + C_{s3} + C_{s4} + C_{banco})\dot{z}_{s\,s} + (-l_d C_{s1} - l_d C_{s2} + l_t C_{s3} + l_t C_{s4} - x_{banco} C_{banco})\dot{\theta}_s \\ & - C_{s1} \dot{z}_{u1} - C_{s2} \dot{z}_{u2} - C_{s3} \dot{z}_{u3} - C_{s4} \dot{z}_{u4} + (-b_{d1} C_{s1} + b_{d2} C_{s2} + b_{t2} C_{s3} - b_{t2} C_{s4} + y_{banco} C_{banco})\dot{\varphi}_s = 0 \end{aligned} \tag{4}$$

$$\begin{aligned}
&I_{xx}\ddot{\varphi}_s + (-b_{d1}K_{s1} + b_{d2}K_{s2} + b_{t2}K_{s3} - b_{t2}K_{s4} + y_{banco}K_{banco})z_s + (l_d b_{d1}K_{s1} - l_d b_{d2}K_{s2} + l_t b_{t2}K_{s3} \\
&- l_t b_{t1}K_{s4} - x_{banco}y_{banco}K_{banco})\theta_s + b_{d1}K_{s1}z_{u1} - b_{d2}K_{s2}z_{u2} - b_{t2}K_{s3}z_{u3} + b_{t1}K_{s4}z_{u4} \\
&+ (b_{d1}^2K_{s1} + b_{d2}^2K_{s2} + b_{t2}^2K_{s3} + b_{t1}^2K_{s4} + y_{banco}^2K_{banco})\varphi_s - y_{banco/}K_{banco}z_{banco} + (-b_{d1}C_{s1} + b_{d2}C_{s2} \\
&+ b_{t2}C_{s3} - b_{t2}C_{s4} + y_{banco}C_{banco})\dot{z}_s + (l_d b_{d1}C_{s1} - l_d b_{d2}C_{s2} + l_t b_{t2}C_{s3} - l_t b_{t1}C_{s4} - x_{banco}y_{banco}C_{banco})\dot{\theta}_s \\
&+ b_{d1}C_{s1}\dot{z}_{u1} - b_{d2}C_{s2}\dot{z}_{u2} - b_{t2}C_{s3}\dot{z}_{u3} + b_{t1}C_{s4}\dot{z}_{u4} + (b_{d1}^2C_{s1} + b_{d2}^2C_{s2} + b_{t2}^2C_{s3} + b_{t1}^2C_{s4} + y_{banco}^2C_{banco})\dot{\varphi}_s \\
&- y_{banco/}C_{banco}\dot{z}_{banco} = 0
\end{aligned} \tag{5}$$

$$\begin{aligned}
&I_{yy}\ddot{\theta}_s + (-l_dK_{s1} - l_dK_{s2} + l_tK_{s3} + l_tK_{s4} - x_{banco}K_{banco})z_s + (l_d^2K_{s1} + l_d^2K_{s2} + l_t^2K_{s3} + l_t^2K_{s4} \\
&+ x_{banco}^2K_{banco})\theta_s + l_dK_{s1}z_{u1} + l_dK_{s2}z_{u2} - l_tK_{s3}z_{u3} - l_tK_{s4}z_{u4} + (l_d b_{d1}K_{s1} - l_d b_{d2}K_{s2} + l_t b_{t2}K_{s3} \\
&- l_t b_{t1}K_{s4} - x_{banco}y_{banco}K_{banco})\varphi_s + x_{banco/}K_{banco}z_{banco} + (-l_dC_{s1} - l_dC_{s2} + l_tC_{s3} + l_tC_{s4} \\
&- x_{banco}C_{banco})\dot{z}_s + (l_d^2C_{s1} + l_d^2C_{s2} + l_t^2C_{s3} + l_t^2C_{s4} + x_{banco}^2C_{banco})\dot{\theta}_s + l_dC_{s1}z_{u1} + l_dC_{s2}z_{u2} \\
&- l_tC_{s3}z_{u3} - l_tC_{s4}z_{u4} + (l_d b_{d1}C_{s1} - l_d b_{d2}C_{s2} + l_t b_{t2}C_{s3} - l_t b_{t1}C_{s4} \\
&- x_{banco}y_{banco}C_{banco})\dot{\varphi}_s + x_{banco/}C_{banco}\dot{z}_{banco} = 0
\end{aligned} \tag{6}$$

$$m_1\ddot{z}_{u1} - K_{s1}z_s + l_dK_{s1}\theta_s + (K_{s1} + K_{p1})z_{u1} + b_{d1}K_{s1}\varphi_s - C_{s1}\dot{z}_s + l_dC_{s1}\dot{\theta}_s + b_{d1}C_{s1}\dot{\varphi}_s + C_{s1}\dot{z}_{u1} = K_{p1}z_{p1} \tag{7}$$

$$m_2\ddot{z}_{u2} - K_{s2}z_s + l_dK_{s2}\theta_s + (K_{s2} + K_{p2})z_{u2} - b_{d2}K_{s2}\varphi_s - C_{s2}\dot{z}_s + l_dC_{s2}\dot{\theta}_s - b_{d1}C_{s2}\dot{\varphi}_s + C_{s2}\dot{z}_{u2} = K_{p2}z_{p2} \tag{8}$$

$$m_3\ddot{z}_{u3} - K_{s3}z_s - l_tK_{s3}\theta_s + (K_{s3} + K_{p3})z_{u3} - b_{t2}K_{s3}\varphi_s - C_{s3}\dot{z}_s - l_tC_{s3}\dot{\theta}_s - b_{t2}C_{s3}\dot{\varphi}_s + C_{s3}\dot{z}_{u3} = K_{p3}z_{p3} \tag{9}$$

$$m_4\ddot{z}_{u4} - K_{s4}z_s - l_tK_{s4}\theta_s + (K_{s4} + K_{p4})z_{u4} + b_{t1}K_{s4}\varphi_s - C_{s4}\dot{z}_s - l_tC_{s4}\dot{\theta}_s + b_{t1}C_{s4}\dot{\varphi}_s + C_{s4}\dot{z}_{u4} = K_{p4}z_{p4} \tag{10}$$

These set of equations were used to generate a routine in MATLAB®, and solve these equations and provide acceleration data of each body system.

The signal utilized to represent the road is a sinusoidal with 0.001m of amplitude and frequency of 5.0265 Hz. The signal of the front and rear of the car were lagged relative to the length of the axles of the car. Whereas the vehicle at a speed of 80 Km/h, is obtained 0.113s of delay. These data were based on Patrício (2005).

3. RESULTS

Table 3 shows the natural frequencies obtained from analytical model and from ADAMS/VIEW®.

Table 3. Natural frequencies of the various components

Bodies	Analytical model – MATLAB® (Hz)	ADAMS/VIEW® (Hz)
Driver Head	8.0433	8.043270
Driver Body	1.5850	1.585240
Seat	9.4309	9.430940
Sprung Mass Bounce	0.9127	0.916406
Sprung Mass Pitch	0.9507	0.946100
Sprung Mass Roll	0.7354	0.733586
Unsprung Mass Bounce	9.1478	9.147820
Unsprung Mass Bounce	9.1457	9.145720
Unsprung Mass Bounce	9.1427	9.142760
Unsprung Mass Bounce	9.1476	9.147570

The natural frequency in ADAMS/VIEW® and MATLAB® values are close, showing error in the third decimal place. Bounce and pitch frequencies are consistent with Patrício (2005). These differences between values obtained both MATLAB® and ADAMS/VIEW® occurs due to differences between the methods of solving matrices of two software's.

ISSN 2176-5480

Griffin (2009) shows that for natural frequencies of the seat from 0.5 to 4 Hz cause discomfort to passengers, because the system amplifies the input offset from the body. The proposed model provided natural frequency of approximately 9.4309 Hz, demonstrating that the seat model offers improved passenger comfort as the system is in the region of attenuation of the excitation input.

Figure 3 shows the Fast Fourier Transform for each displacement signal for each part which composes the model obtained for MATLAB®. At a certain frequency vibration mode of a certain part of the model is excited. The points marked on the graph correspond to the natural frequencies of each part found both in MATLAB® and in ADAMS/VIEW®. However, it is clear that the modes of vibration are excited along other parts of the body which enter in resonance, as can be seen that there are several peaks in the same frequency.

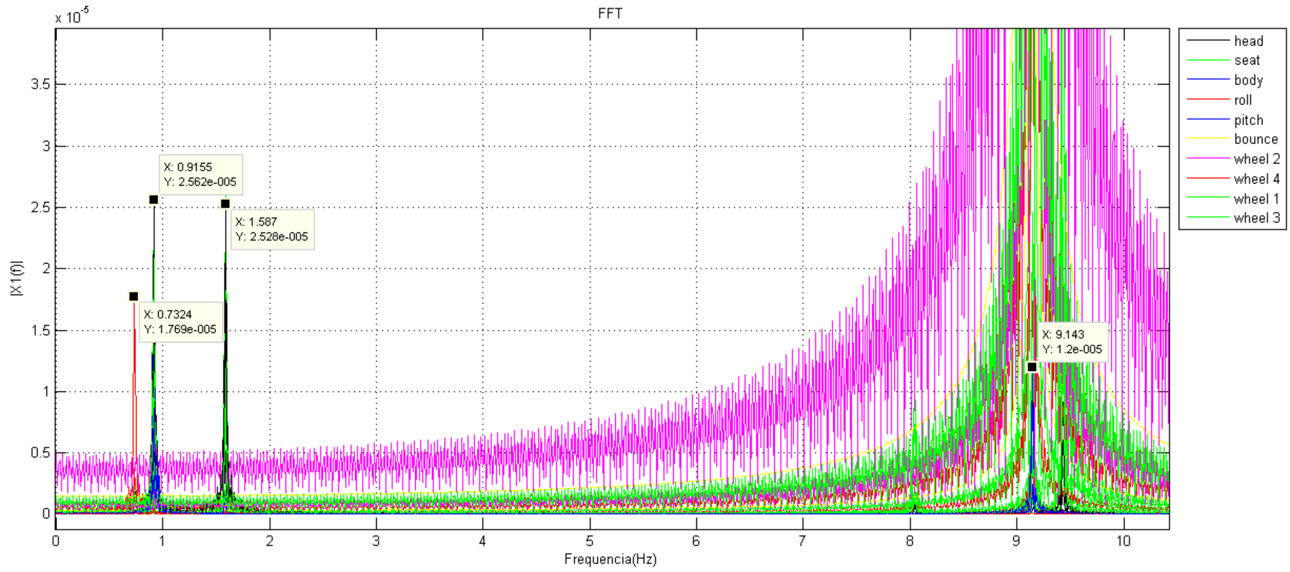

Figure 3. Fast Fourier Transform for each displacement signal for each part which composes the model

The difference between the natural frequencies obtained by (Patrício, 2005) was on sprung mass roll that is 2.34 Hz. This difference is due the anti-roll bar that was not considered in this work.

The figure 4 and 5 above shows the acceleration in the driver head respectively in MATLAB® and ADAMS/VIEW®.

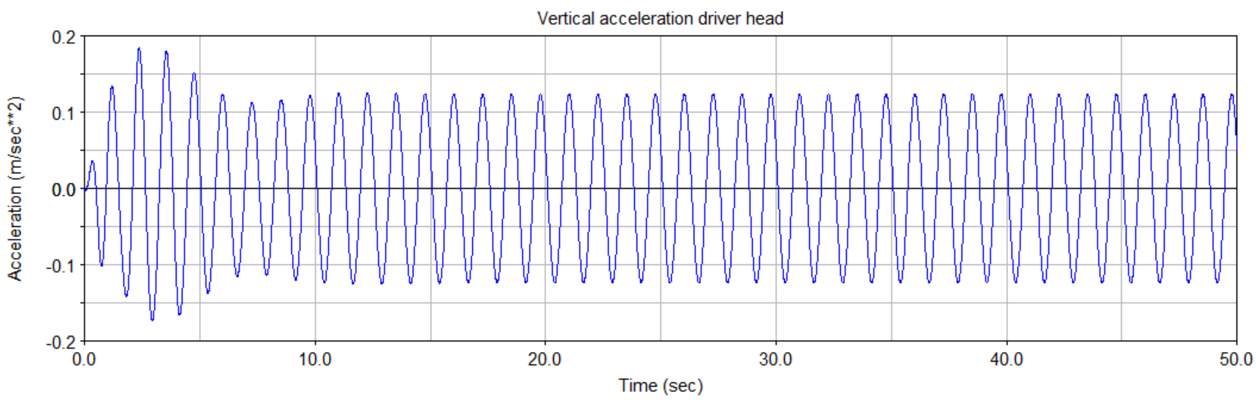

Figure 4. Vertical acceleration in driver head – ADAMS/VIEW®

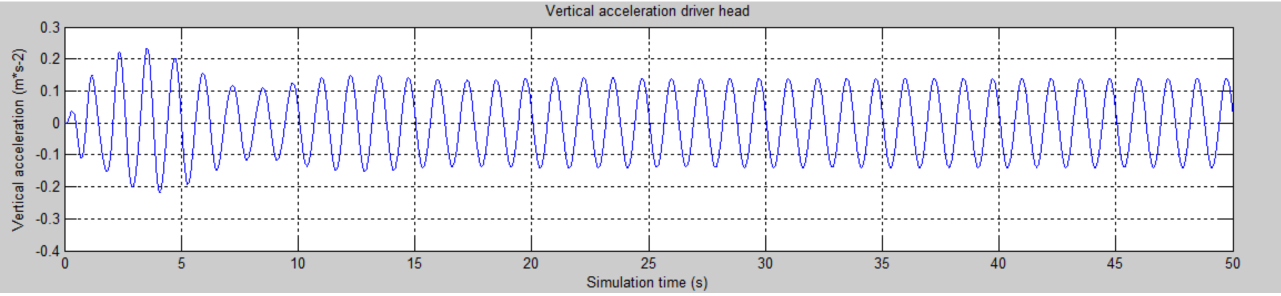

Figure 5. Vertical acceleration in driver head - MATLAB®

The acceleration signal in the driver's head starts with a higher amplitude due to the fact of the front axle suffer the impact of the first track and consequently transmit to the driver. After the damping of the human body works and the amplitude goes steady-state. Both software provided similar curves, and enter in steady-state after 10 seconds.

Figures 6 and 7 show the vertical acceleration at the seat obtained respectively in MATLAB® and ADAMS/VIEW®.

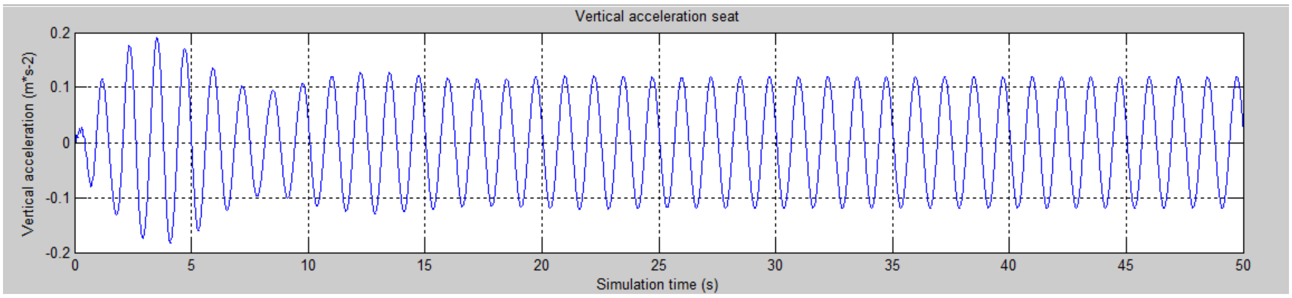

Figure 6. Seat vertical acceleration/MATLAB®

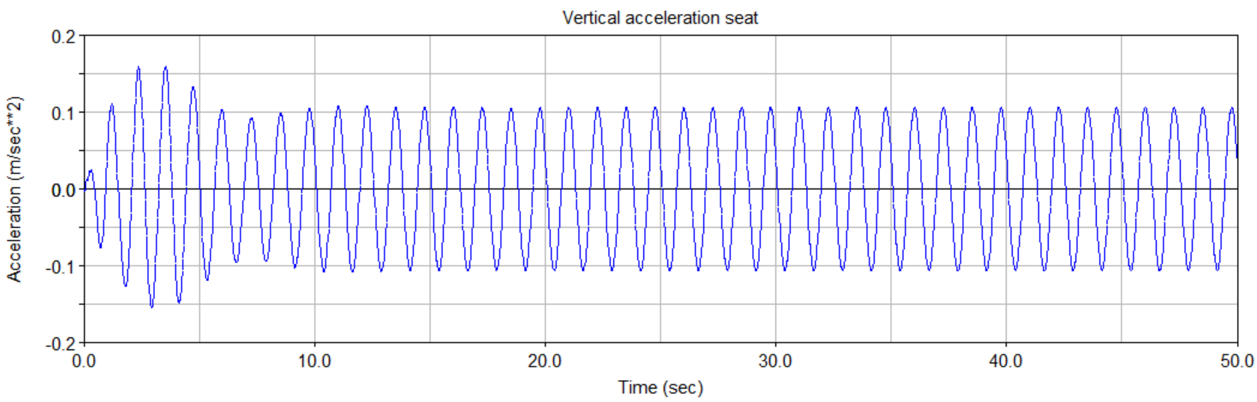

Figure 7. Seat vertical acceleration/ADAMS/VIEW®

According Griffin (2009) the acceleration level in seat varies between 0.1 to 0.450 m/sec^2 for an excitation that will not prejudice the health of the passenger, for a limit of 24 hours exposition. The purpose model obtained acceleration level of 0.121 m/sec^2 in seat for steady-state, as can be seen by comparing the figures 6 and 7. This curve can be used to analyze driver comfort. This work does not consider values of stiffness of the body and the head because the primary objective is verify that the proposed model in MATLAB® and in ADAMS/VIEW® converges to the same solution.

Figures 8 and 9 shows sprung mass roll angle signal obtained by MATLAB® and ADAMS/VIEW®.

ISSN 2176-5480

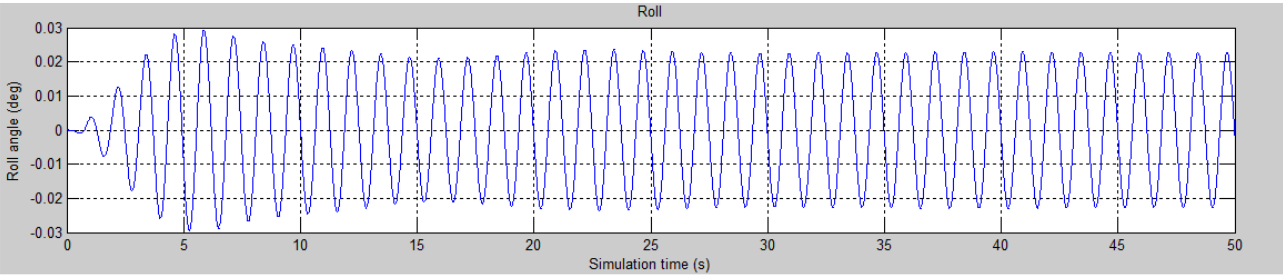

Figure 8. Sprung mass roll/MATLAB®

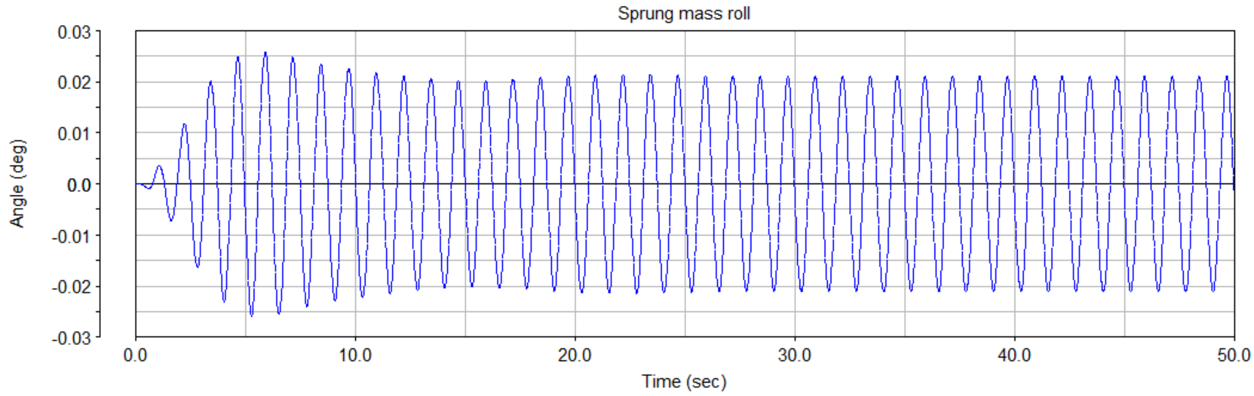

Figure 9. Sprung mass roll/ADAMS/VIEW®

The roll angles are small because there is no difference of height between wheels on the same axle, but the roll axis of the vehicle coincides with the sprung mass C.G. by causing appearance of a moment that can cause roll of the body. The roll angle variation, peak to peak is about 0.04 degrees. Patricio (2005) obtained the same values but it enters in steady state faster because of the anti-roll bar.

Figures 10 and 11 shows sprung mass pitch angle signal obtained in MATLAB® and ADAMS/VIEW®.

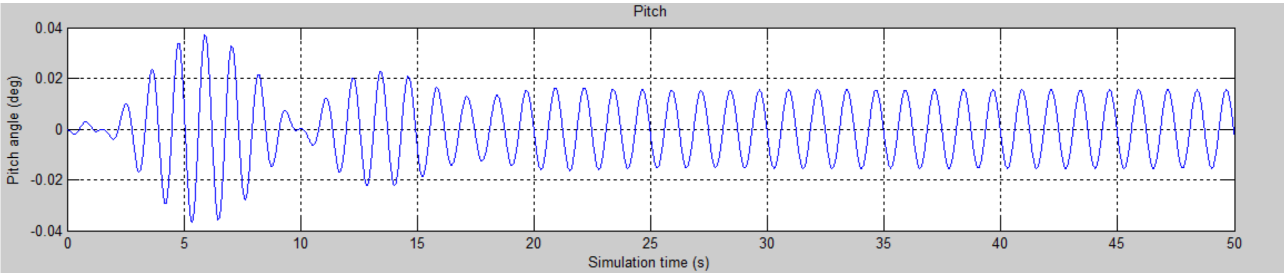

Figure 10. Sprung mass pitch/MATLAB®

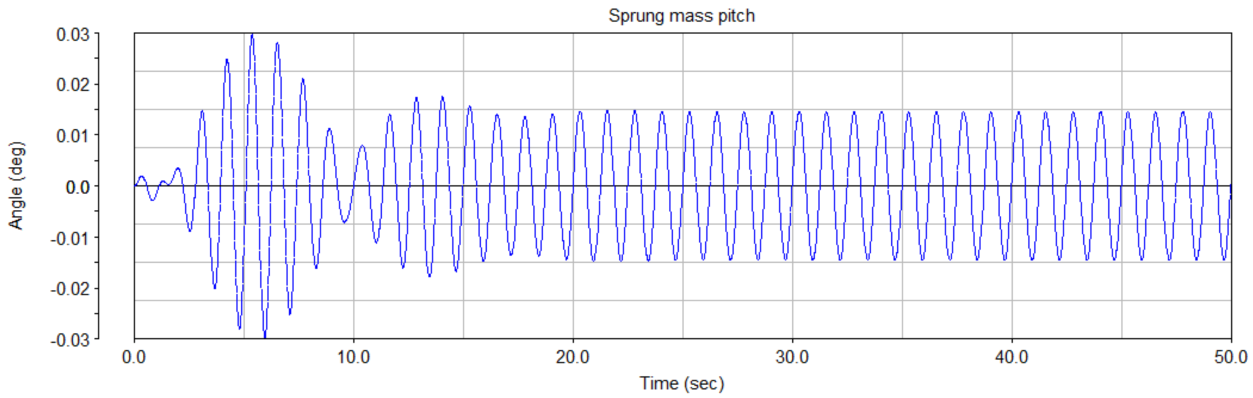

Figure 11. Sprung mass pitch/ADAMS/VIEW®

ISSN 2176-5480

Pitch initial amplitude is higher because the front axle is excited first by the road, and the rear axle is excited only after the delay time. This amplitude is attenuated by action of the damper. The vehicle will go through a sequence of peaks and valleys of the sine wave generated by the road, and the system takes longer to enter in steady-state.

The pitch angles has low amplitude variation, approximately 0.03 degrees peak-to-peak, because the amplitude of the sinusoid which simulates the pavement is low.

Figures 12 and 13 shows sprung mass bounce signal obtained in MATLAB® and ADAMS/VIEW®.

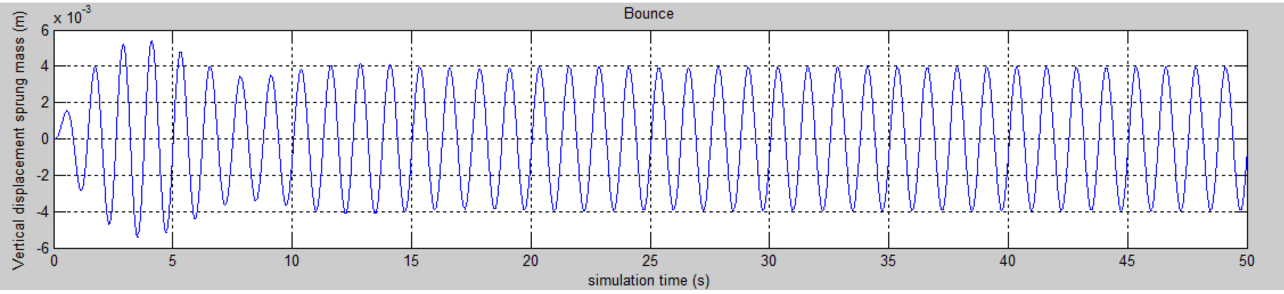

Figure 12. Sprung mass bounce/MATLAB®

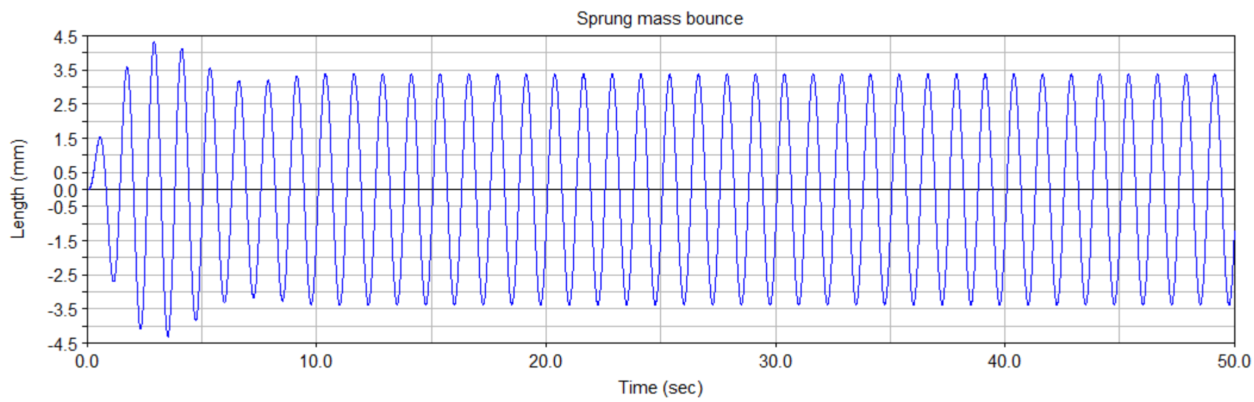

Figure 13. Sprung mass bounce/ADAMS/VIEW®

Thought bounce curves can be perceived the action of damping to absorb the spring energy and reduce the amplitude when the vehicle goes thought the first peak of the sinusoid, and after 10 seconds enters in steady state. The damper operates even when the tendency of the system is to amplify as can be seen in Figure 14 by the transmissibility curve and gain value of sprung mass bounce provided by table 5.

Table 4 shows the peak values in steady-state of the curves obtained in MATLAB® and ADAMS/VIEW® for a vertical acceleration of the seat and driver's head, and displacement of bounce, pitch and roll.

Thought the comparison of steady state peak values between ADAMS/VIEW® and MATLAB® can be seen a difference show in the table 4. This error can be caused because the difference of solution utilized by the softwares.

Table 4. Error values of curves obtained in MATLAB® and ADAMS/VIEW®

Curve	Error
Acceleration in driver head (m*sec^2)	12.49 %
Acceleration in seat (m*sec^2)	11.85%
Sprung mass bounce (mm)	-13.72%
Sprung mass pitch (deg)	7.88%
Sprung mass roll (deg)	6.25%

Figure 14 shows the transmissibility curves of the vertical displacement of the wheels and bounce of the sprung mass relative to the excitement of the pavement.

ISSN 2176-5480

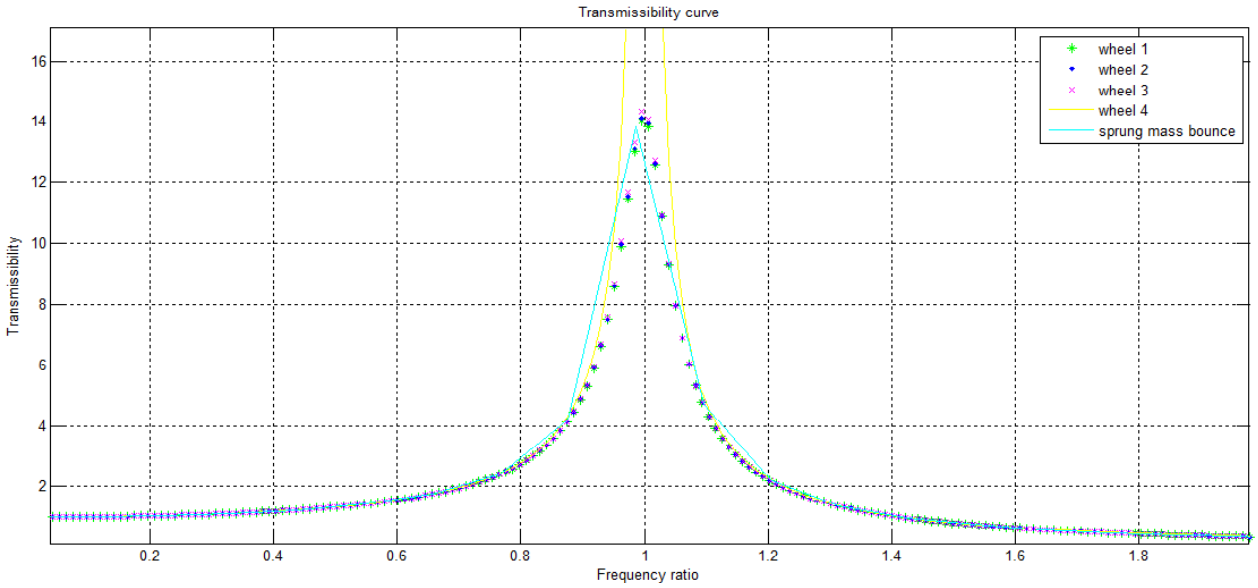

Figure 14. Transmissibility curves

Table 5 shows frequency ratio values that were in the amplification region, and can be seen the gain through the ratio of input amplitude (pavement) and output amplitude (wheels vertical displacement and sprung mass bounce).

Table 5. Comparison between vertical displacement amplitude in MATLAB® and ADAMS/VIEW ®

	Pavement Frequency (Hz)	Natural frequency in MATLAB® (Hz)	Frequency ratio	Gain	Amplitude (mm) in MATLAB®	Amplitude (mm) in ADAMS/VIEW®
Left front wheel	0.8	9.1476	0.087	1.1	1.31	1.25
Right front wheel	0.8	9.1457	0.087	1.1	1.31	1.25
Left rear wheel	0.8	9.1428	0.088	1.1	1.31	1.25
Right rear wheel	0.8	9.1478	0.087	1.1	1.31	1.25
Sprung Mass Bounce	0.8	0.9127	0.88	4.18	3.928	3.3986

4. CONCLUSIONS

The model proposed presents the highest error between MATLAB® and ADAMS/VIEW® lower than 14% in relation of the acceleration curves and displacement of the sprung mass. Both model obtained similar curves and can represent the model. The difference between were their due difference of the assembly of the program, i.e., the routine of solution of the software's. It is known that the error is propagated, and the sprung mass pitch and bounce is the only who suffer the greater influence because the method solution of the equations of motion is different.

The natural frequencies were practically the same, the error between the methods were less 1%. Therefore, the method used on MATLAB®, matrices manipulation, propagates fewer errors and the method used on ADAMS/VIEW® is reliable.

The transmissibility curve is an important tool for the conference of how much is transmitted as movement of a body relative to another. The curves gain of the vertical displacement of the wheels and the body, at steady state in relation to the road can be input through the transmissibility curve. It showed consistent in both software.

5. ACKNOWLEDGEMENTS

The authors thank FAPEMIG and CAPES for support.

ISSN 2176-5480

6. REFERENCES

Blundell M., Harty D., “Multibody Systems Approach to Vehicle Dynamics”, 2ed, Elsevier, Burlington,2004.

Bouazara, M., Richard, M. J., 2001. “An optimization method designed to improve 3-D vehicle comfort and road holding capability through the use of active and semi-active suspensions”. *European Journal Mechanics A/Solids*, v.20, n.3, p. 509-520

Dukkipati, R. V., Pang, J., Qatu, M. S., Sheng, G., Shuguang, Z., “Road Vehicle Dynamics”, SAE International, Warrendale, 2008.

Genta, G., Morello L., "The Automotive Chassis Volume 2 System Design", Springer, 2009

Gillespie T. D. “Fundamentals of Vehicle Dynamics” SAE, 1992.

Griffin, M. J., "Handbook of human vibration", Academic Press, San Diego, 1990

Reimpell, J., Stoll, H., Betzler, J. W., "The Automotive Chassis: Engineering Principles, Elsevier, Woburn, - Butterworth-Heinemann, 2ed, 2001.

Stone, R., Ball J. K., " Automotive Engineering Fundamentals", SAE International, Warrendale,2004

Patrício, L. F., ”Desenvolvimento matemático e implementação numérica de um modelo tridimensional para determinação das respostas dinâmicas de um veículo automotor” Dissertação (Mestrado em Engenharia Mecânica) – Pontifícia Universidade Católica de Minas Gerais, Programa de Pós-Graduação em Engenharia Mecânica, 2005 Belo Horizonte.

Wong J. Y. - Theory of ground vehicles – 2001.

7. RESPONSIBILITY NOTICE

The authors are the only responsible for the printed material included in this paper.